Talanta 82 (2010) 1701–1707

Contents lists available at ScienceDirect

Talanta

journal homepage: www.elsevier.com/locate/talanta

Zirconia layer coated mesoporous silica microspheres used for highly specific phosphopeptide enrichment

Huihui Wan, Jingyu Yan, Long Yu, Xiuli Zhang, Xingya Xue, Xiuling Li*, Xinmiao Liang**

Key Lab of Separation Science for Analytical Chemistry, Dalian Institute of Chemical Physics, Chinese Academy of Sciences, 457 Zhongshan Road, Dalian, China

ARTICLE INFO

Article history:
Received 19 May 2010
Received in revised form 19 July 2010
Accepted 22 July 2010
Available online 30 July 2010

Keywords:
Phosphopeptide enrichment
Zirconia layer
Mesoporous silica
ESI-Q-TOF

ABSTRACT

Zirconia layer coated mesoporous silica microspheres with mesostructured cellular foams (MCFs) were prepared by NH_3/water vapor-induced internal hydrolysis method. Zirconia layer coated MCF microspheres were characterized by SEM, XRD, N_2 sorption, UV, and chromatographic analysis, and explored for enrichment of phosphopeptides. ZrO_2/MCF microspheres in solid-phase extraction (SPE) mode demonstrated much higher selectivity and higher efficiency towards phosphopeptide enrichment than bulk ZrO_2 particles. In particular, the selectivities of ZrO_2/MCF microspheres towards multi-phosphopeptides are even higher than that of the widely used commercial TiO_2 microparticles. The ZrO_2/MCF microspheres were also applied to enrich endogenous phosphopeptides from human serum, and twelve endogenous phosphorylated peptides could be specifically enriched.

1. Introduction

Protein phosphorylation is recognized as one of the most important post-translational modifications (PTMs), which involves in a large number of biological processes, such as cellular growth migration, differentiation, intercellular communication and metabolisms. Characterization of the phosphorylation sites of the proteins is crucial for understanding the role of protein phosphorylation in these biological processes [1–3]. However, the low abundance and sub-stoichiometric modification-site occupancy of PTMs can result in lessened ion signals of the phosphorylated peptides in mass spectrometry (MS) analysis, which will be suppressed by the large excess of non-phosphorylated peptides in protein digests. Therefore, a specific enrichment step targeting phosphopeptides from peptide mixture is prerequisite before MS analysis [4]. Considerable efforts, including immunopurification through phosphoprotein antibody [5,6], strong cation chromatography [7,8], strong anion chromatography [9], and affinity chromatography, have been expended to develop methods for the isolation of phosphopeptides aiming at the phosphate functional groups. Commonly used affinity based method is immobilized metal ion affinity chromatography (IMAC) [10–12] using Fe(III), Ga(III), or other metals. However, nonspecific binding of non-phosphorylated acidic peptides and the complexity of factors affecting phosphopeptide binding and release often result in low specificity for target phosphopeptides. Recently, phosphopeptide-enrichment strategies, based on metal oxide affinity chromatography (MOAC), have been widely used in large-scale phosphoproteome due to the specific and reversible affinity of phosphate groups to the amphoteric surface of metal oxides [13–18]. Microparticles of titanium dioxide (TiO_2) [13–15], zirconium oxide (ZrO_2) [16], aluminum hydroxide ($Al(OH)_3$) [17] and other metal oxides [18] have been explored in phosphopeptide isolation and exhibited higher specificity for trapping phosphate groups than IMAC. However, the relatively low surface areas of these microparticles limit their applications. Owning to their potential higher surface areas than particles of microscale, titania-coated magnetic iron oxide (Fe_3O_4@TiO_2) [19], and ZrO_2 nanoparticles [20], have been attempted by centrifugation and demonstrated higher capacities to trap phosphopeptides.

Mesoporous materials possess of unique textural properties, such as high surface area, flow-through ordered structure and narrow pore size distribution. Such large surface areas, together with the many active surface sites, can be translated into even higher loading capacity for binding phosphate groups. Mesoporous MCM-41 silica nanoparticles immobilized with titanium ion have been used to selectively capture phosphopeptides from complex peptide and protein mixtures with high sensitivity based on MALDI-TOF-MS detection, and four phosphorylated peptides from serum samples can be observed after enrichment with Ti(IV)-MCM-41 [21]. Very recently, ZrO_2 nanoparticles with mesoporous structure have demonstrated higher selectivity than commercial

* Corresponding author at: Dalian Institute of Chemical Physics, Bio-technique Department, 457 Zhongshan Road, Dalian, Liaoning 116023, China.
Tel.: +86 411 84379523.
** Corresponding author at: Dalian Institute of Chemical Physics, Bio-technique Department, 457 Zhongshan Road, Dalian, Liaoning 116023, China.
Tel.: +86 411 84379519; fax: +86 411 84379539.
E-mail addresses: lixiuling@dicp.ac.cn (X. Li), liangxm@dicp.ac.cn (X. Liang).

0039-9140/$ – see front matter © 2010 Elsevier B.V. All rights reserved.
doi:10.1016/j.talanta.2010.07.050

ZrO_2 microparticles for phosphopeptide enrichment [22]. However, the co-sedimentation of peptides in centrifugation procedure and large elution volumes embarrassed the nanoparticle efficiency in phosphopeptide enrichment. Therefore, metal oxide microparticles with high surface area which can be used in columns or tips are desired for phosphopeptide analysis. However, most of synthesized mesoporous ZrO_2 is thermal instability and will collapse by calcination at high temperatures, and it is challenging to control the morphology of the mesoporous ZrO_2 to obtain micro particles. Therefore, supporting zirconia on mesoporous silica microspheres is an alternative way to improve its dispersion and hence the surface area.

Due to the interfacial electronic and structural interactions between the metal oxide and silica support, the structural features and physical-chemistry properties of metal oxide layer in highly dispersed state on the surface of silica supports differ greatly to that of the bulk crystalline metal oxides [23–25]. Furthermore, these metal oxides dispersed mesoporous oxide materials can preserve the unique textural properties. Therefore, these metal oxides dispersed oxide materials have been widely applied as catalysis, separation, adsorption and host materials [26–29]. TiO_2 modified macroporous silica foams demonstrated higher efficient and sensitive phosphopeptide enrichment than TiO_2 nanoparticles. Based on the strong affinity of 4-coordinated Ti^{IV} species for the phosphate group, the highly dispersed Ti^{IV} species on the silica surface showed preferential enrichment of multi-phosphorylated peptides with very low detection limit and high selectivity [30]. Micrometer-sized three-dimensional siliceous mesostructured cellular foam (MCF) [31,32] spheres with large pore size have been synthesized and used as packing materials in high-performance liquid chromatography [33,34]. However, the ordered structure could be destroyed by the formation of bulk crystalline metal oxide, which puzzled high loadings of metal oxide on the surface of mesoporous silica [29]. Ogura and coworkers have recently resolved this disturbance and coated high loading of ZrO_2 on the surface of mesoporous SBA-15 silica without pore blocking by NH_3/water vapor-induced internal hydrolysis method [35].

In this study, zirconia layer coated MCF silica microspheres were synthesized and characterized thoroughly. The zirconia layer coated mesoporous MCF silica ZrO_2/MCF microspheres were explored in solid-phase extraction (SPE) mode to enrich phosphopeptides from standard tryptic protein digests, and further used for enrichment of the endogenous phosphopeptides from human serum.

2. Experimental

2.1. Chemicals and reagents

The following reagents were used: toluene, NH_3/H_2O (25%), pyridine, and acetone (analytical grade) from Tianjin Kermel (Tianjin, China); methanol from Shandong Yuwang Chemicals (Dezhou, China); dimethyloctadecylchlorosilane from Alfa-Aesar (Ward Hill, MA, USA); trifluoroacetic acid (TFA) from Dima Technology Inc. (Richmond Hill, USA); α-casein, ammonium bicarbonate, and lactic acid (LA) from Sigma–Aldrich (St. Louis, MO); trypsin (sequencing grade) from Promega (Madison, WI); formic acid (FA) from Acros (Geel, Belgium); acetonitrile (CH_3CN) from Merck (Darmstadt, Germany); urea from Shenyang Lianbang Chemicals (Shenyang, China); 3-hydroxypropionic acid (HPA) from TCI Chemicals (Japan); NH_3/H_2O (10%) from Fluka (Switzerland); TiO_2 from GL Sciences (Japan); GELoader tips from Eppendorf (Hamburg, Germany); and C18-AQ from Sunchrom (Friedrichsdorf, Germany). All the water used in experiments was purified using a Milli-Q system (Millipore, Bedford, MA, USA).

2.2. Synthesis and characterization of ZrO_2(12, 24)/MCF

2.2.1. Synthesis of ZrO_2(12, 24)/MCF

Mesoporous MCF silica particles were synthesized according to published procedure [36] and our previous work [34]. Synthesis of ZrO_2/MCF was according to published NH_3/water vapor-induced internal hydrolysis method [35]. Briefly, 12% (m/m) ZrO_2 equivalent of precursor of $ZrO(NO_3)_2{\cdot}2H_2O$ was wet-impregnated into the pores of MCF silica under stirring at 60 °C until dryness, and then further heated at 100 °C for 6 h. By repeating the above procedures, 24% (m/m) zirconia equivalent of precursor of $ZrO(NO_3)_2{\cdot}2H_2O$ impregnated MCF can be obtained. The zirconia precursor loaded MCF silica (1.0 g) was put in an open glass and kept inside the autoclave which contained a 14% ammonium hydroxide (20 mL) without contact with the ammonium hydroxide. The sample was heated at 100 °C for 12 h and calcined under air at 500 °C for 5 h. Then ZrO_2(12, 24)/MCF materials were obtained, where 12 and 24 represents the % (m/m) of ZrO_2 loaded into the MCF spheres.

2.2.2. Characterization of ZrO_2(12, 24)/MCF

Scanning electron microscopy (SEM) images were taken on a HB-600 electron microscope with an accelerating voltage of 25 kV. Powder X-ray diffraction (XRD) was performed on a Rigaku D/max 3400 diffractometer (Cu Kα radiation, λ = 0.1542 nm) at 20 kV and 50 mA. N_2 adsorption–desorption experiments were undertaken isothermally at 77 K on an automatic ASAP 2000 Micromeritics apparatus. Prior to measurement, the materials were out-gassed at 573 K for 10 h. BET surface areas were calculated from adsorption data in the relative pressure range from 0.01 to 0.2. The total pore volume was evaluated at a relative pressure about 0.99. Pore size distributions were analyzed with the supplied BJH software package from the adsorption branches of the isotherms. Ultraviolet–visible diffuse reflectance spectrum was recorded on a JASCO V-550 UV–visible spectrophotometer. The Van Deemter chromatographic experiments were performed on the HPLC system (Agilent 1100 Series, USA) consisted of a quaternary pump, an auto-sampler, a degasser, an automatic thermostatic column compartment, and a diode array UV detector.

2.3. Phosphopeptide enrichment

2.3.1. Trypsin digestion of α-casein

1 mg α-casein was dissolved in 1 mL of ammonium bicarbonate (50 mM, pH 8.0) and digest in trypsin for 18 h at 37 °C with a 1:40 (w/w) enzyme-to-protein ratio.

2.3.2. Phosphopeptide enrichment from standard phosphoprotein digests

250 μg of ZrO_2(12, 24)/MCF and MCF beads, 1 mg of TiO_2, or 500 μg of ZrO_2 beads were packed in GELoader tips, respectively. The ZrO_2(12, 24)/MCF, MCF, and ZrO_2 tips were equilibrated with 20 μL of 100 mg/mL 3-hydroxypropionic acid (HPA) in 0.1% TFA/80% CH_3CN and then 1 μL of α-casein digested solution was loaded on the ZrO_2/MCF, MCF and TiO_2 tips. After successive washing with 20 μL of 100 mg/mL HPA in 0.1% TFA/80% CH_3CN and 20 μL of 0.1% TFA/80% CH_3CN, the bound phosphopeptides were eluted with 20 μL of 2% ammonium hydroxide. For TiO_2 tips, 100 mg/mL HPA was replaced to 300 mg/mL lactic acid. The eluted solution was acidified with 10% FA and desalted with C_{18} microcolumns before ESI-Q-TOF-MS analysis.

2.3.3. Endogenous phosphopeptide enrichment from human serum

1 mg of ZrO_2(12)/MCF was slurried in 100 μL of 0.1% TFA/80% CH_3CN, packed onto SPE microcolumn, and then equilibrated with 90 μL of 100 mg/mL HPA in 0.1% TFA/80% CH_3CN. An aliquot

(700 μL) of human serum was diluted to 2.8 mL of solution with 100 mg/mL HPA in 0.1% TFA/80% CH_3CN, vibrated for 2 min, and centrifuged at 15 000 × *g* for 10 min. The supernatant was collected and loaded onto SPE microcolumns packed with ZrO_2(12)/MCF. The microcolumn was washed sequentially with 250 mM NaCl (120 μL × 2), 100 mg/mL HPA in 0.1% TFA/80% CH_3CN (90 μL × 2), 0.1% TFA/80% CH_3CN (90 μL × 2), 0.1% TFA/50% CH_3CN (90 μL), and 0.1% TFA (90 μL). The bound phosphopeptides were eluted with 2% ammonium hydroxide (40 μL × 2). The eluted solution was acidified with 10 μL of 40% FA, desalted with C_{18} microcolumn. The eluate from C_{18} with 20 μL 0.1% FA/50% CH_3CN was concentrated before nano-RPLC-ESI-Q-TOF-MS analysis.

2.3.4. Desalting

C18-AQ (Sunchrom) material (about 1 mg) was slurried in 30 μL 0.1% FA/80% CH_3CN and packed into GELoader tips. The tips were washed with 40 μL 0.1% FA/80% CH_3CN and 40 μL 0.1% FA. Then tryptic α-casein digests (1 μL), and the neutralized phosphopeptide elution fraction were loaded onto the column, respectively. For tryptic α-casein sample, after rinsing with 40 μL 0.1% FA, the peptide fraction was eluted with 10 μL 0.1% FA/50% CH_3CN, collected, and 5 μL of solution was injected dirctly for ESI-Q-TOF-MS analysis. For phosphopeptide elution from human serum, after rinsing with 60 μL 0.1% FA, the peptide fraction was eluted with 20 μL 0.1% FA/50% CH_3CN, collected, and concentrated for ESI-Q-TOF-MS analysis.

2.4. Nano-ESI-MS and nano-RPLC-ESI-MS analysis

MS experiments were performed on an X'TremeSimple™ nono-LC system (Micro-Tech Scientific, Vista, CA) coupled to a quadrupole time-of-flight (Q-TOF) mass spectrometer (Waters, Manchester, UK). To analyze phosphopeptides enriched from human serum, dried eluate redissolved in 5 μL 0.1% FA/H_2O was loaded onto a C_{18} trap column (10 mm × 150 μm I.D., 3 μm, Micro-Tech Scientific, Vista, CA) at a flow rate of 3 μL/min. After valve switch, the trap column was connected to the C_{18} analytical column (150 mm × 150 μm I.D., 3 μm, Micro-Tech Scientific, Vista, CA) to perform RPLC separation. For RPLC separation, solvent A was 0.1% FA/H_2O and solvent B was 0.1% FA/CH_3CN. The gradient was used: 0 min 5% B; 5 min 12% B; 105 min, 43% B; 106 min, 95% B; 110 min, 95% B; 114 min, 5% B; 120 min, 5% B. The flow rate was set at 1 μL/min. Mass spectrometric experiments were performed under positive-ion survey mode with nanospray voltage at 2.0 kV. MS data were acquired at *m*/*z* 500–2000 for MS analysis and *m*/*z* 100–2000 for MS/MS analysis. The PeptideMass program (http://www.expasy.org/) was employed to calculate the theoretical ions resulting from tryptic digestion of proteins. The data obtained using nanoLC-ESI-MS/MS were processed using Proteinlynx (Waters, Manchester, UK).

3. Results and discussion

3.1. Characterization of ZrO_2(12, 24)/MCF microspheres

Scanning electron microscopy images (Fig. S1) revealed that ZrO_2(12, 24)/MCF samples preserved similar morphology to that of mesoporous silica particles. The small angle X-ray diffraction patterns of the ZrO_2(12, 24)/MCF samples (Fig. S2) and N_2 sorption experiments (Fig. 1) testified that the mesoporous structure is not degraded after coating with zirconia on the surface of mesoporous silica particles, and zirconia has been uniformly dispersed on the surface of mesoporous silica particles without blocking of mesopores. Table S1 illustrates surface area, pore volume and pore diameter calculated by adsorption analysis.

Wide-angle X-ray diffraction patterns of the ZrO_2(12, 24)/MCF samples (Fig. 2) proved that the zirconia layer coated on the pore walls was amorphous in nature. UV–visible diffuse reflectance spectra of the ZrO_2(12, 24)/MCF (Fig. 3) implied further that the zirconium ions were well dispersed in the surface of mesoporous silica. An absorption band at 230 nm accompanied due to O^{2-} to Zr^{4+} charge-transfer transitions can be observed for pure ZrO_2, suggesting that the zirconium atom is in an octahedral coordination. For ZrO_2(12, 24)/MCF samples, only absorbance band at 206 nm corresponding to the O^{2-} to Zr^{4+} charge-transfer transition of highly dispersed Zr^{4+} ions present in an isolated tetrahedral environment can be observed. Therefore, comparison of the bands from the zirconia layer coated mesoporous silica samples with that from reference zirconia, which has a band at 230 nm due to full connectivity of Zr–O–Zr linkages, reveals that zirconia species highly

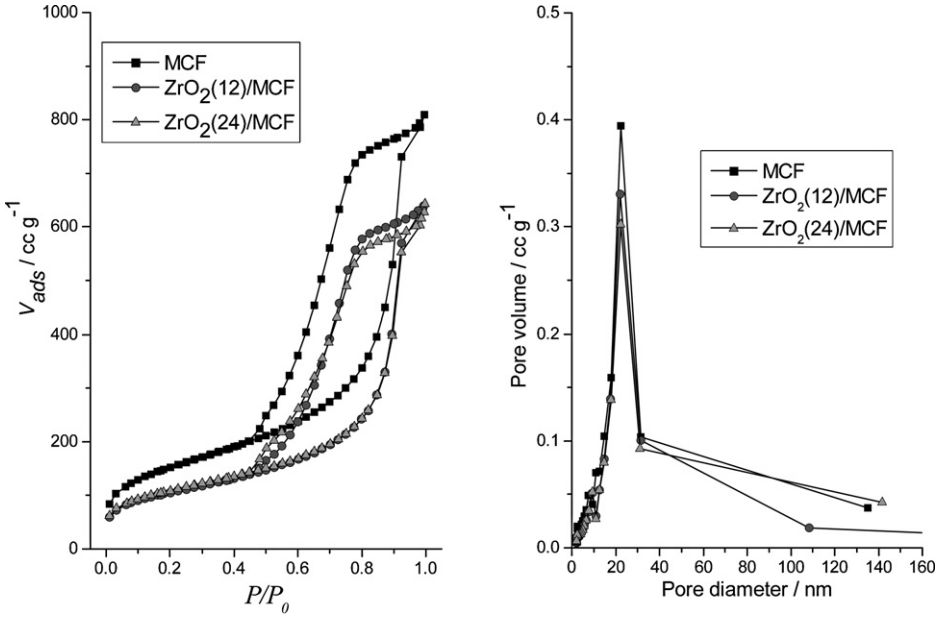

Fig. 1. Nitrogen adsorption–desorption isotherm plots (left) and pore size distribution curves from the adsorption branch (right) of MCF, ZrO_2(12)/MCF, and ZrO_2(24)/MCF. P/P_0 is partial pressure.

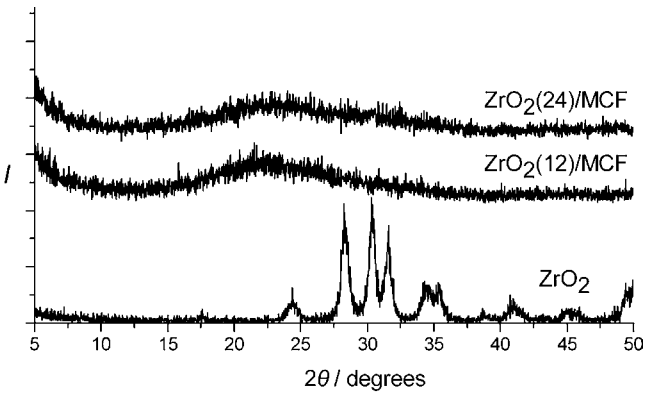

Fig. 2. Wide-angle X-ray diffraction patterns of the MCF, ZrO_2(12)/MCF, and ZrO_2(24)/MCF.

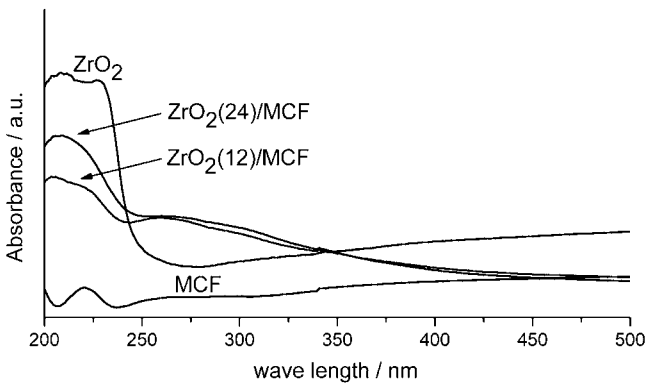

Fig. 3. UV–visible diffuse reflectance spectra of the MCF, ZrO_2(12)/MCF, and ZrO_2(24)/MCF.

dispersed on the mesoporous silica surface are present in coordinatively unsaturated states [35].

3.2. Phosphopeptide-enrichment measurement

3.2.1. Phosphopeptide enrichment from standard phosphoprotein digests

Due to high surface area and high-dispersed coordinatively unsaturated Zr^{IV} species, $ZrO_2(x)$/MCF materials may show unique property for binding phosphopeptides. To investigate the selectivity and efficiency of ZrO_2(12, 24)/MCF materials for the isolation of phosphopeptides, a standard phosphoprotein, α-casein [22,37] was selected because of its well characterized phosphorylation sites. The spherical morphology of ZrO_2/MCF material makes it feasible to perform enrichment in SPE mode, which has been proved by the Van Deemter chromatographic experiments (Fig. S3) with high column efficiency and mechanically stability for C_{18}–ZrO_2(24)/MCF

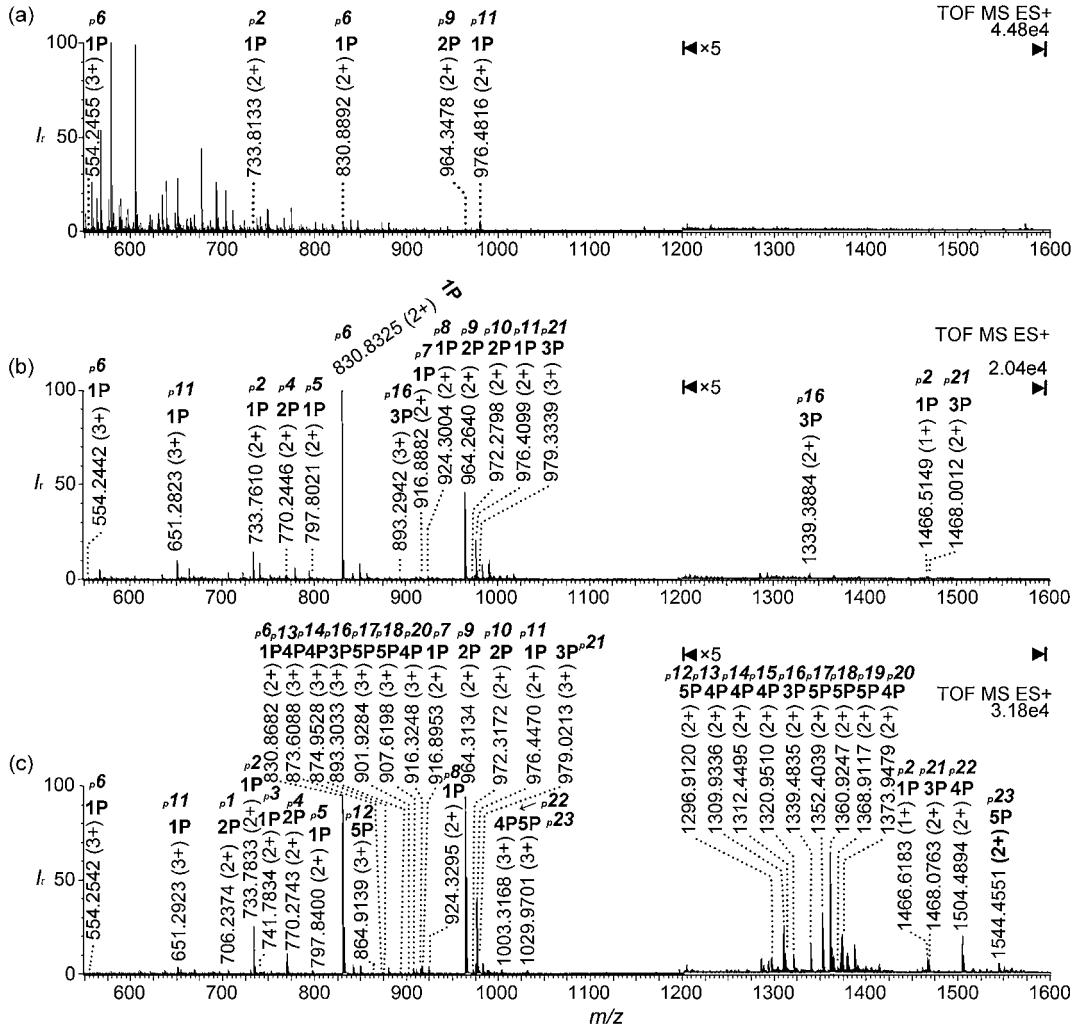

Fig. 4. Nano-ESI-TOF mass spectra for tryptic α-casein digests (a) desalted with C_{18}; enriched by (b) 1 mg of commercial TiO_2, and (c) 250 μg of ZrO_2(12)/MCF. P indicates phosphate group.

microspheres. The ESI-MS spectra of tryptic digested α-casein desalted with C_{18} and phosphopeptides eluted from ZrO_2(12)/MCF, and commercial TiO_2 microspheres, are shown in Fig. 4. The MS spectrum of α-casein digests desalted with C_{18} shows that phosphopeptide signals were rather weak due to the ion suppression of the co-eluted non-phosphopeptides, and only 4 phosphopeptides can be detected (Fig. 4a). Among the metal oxides that have been used for the enrichment of phosphopeptides and phosphoproteins, commercial TiO_2 microspheres are the most widely used and have demonstrated high affinity and good selectivity towards phosphopeptides [38]. Here, under optimized loading and washing condition [39,40], 12 phosphopeptides including 6 single-phosphorylated peptides and 6 multi-phosphopeptides can be resolved in the mass spectrum of lactic acid-modified TiO_2 (1 mg) elution fraction (Fig. 4b). Due to the high surface area of ZrO_2(12)/MCF, the enhanced amount of the phosphopeptide adsorption sites of ZrO_2(12)/MCF may show high efficiency for phosphopeptide enrichment. Compared TiO_2 microspheres with 10% ammonium hydroxide solution to release phosphopeptides, phosphopeptides bound on 3-hydroxypropionic acid-modified ZrO_2(12)/MCF could be eluted effectively by 2% ammonium hydroxide solution. 250 μg of ZrO_2(12)/MCF shows enhanced significantly enrichment selectivity for phosphopeptides, especially for multi-phosphorylated peptides. Totally 23 phosphorylated peptides including both 7 mono- and 16 multi-phosphopeptides can be clearly detected in elution fractions from ZrO_2(12)/MCF (Fig. 4c, Table S2).

To elucidate clearly the excellent selectivity and efficiency of ZrO_2/MCF material for phosphopeptide enrichment, 250 μg of MCF silica, 500 μg of ZrO_2 particles calcined from $ZrO(NO_3)_2$, and 250 μg of ZrO_2(24)/MCF were utilized to enrich phosphopeptides from tryptic α-casein digests. The ESI-MS spectra of phosphopeptides eluted from different materials are shown in Fig. 5. Only 4 low-intensity phosphopeptides together with majority of non-phosphopeptides are detected from the elution fraction of pure MCF silica, suggesting non-selective adsorption behavior of phos-

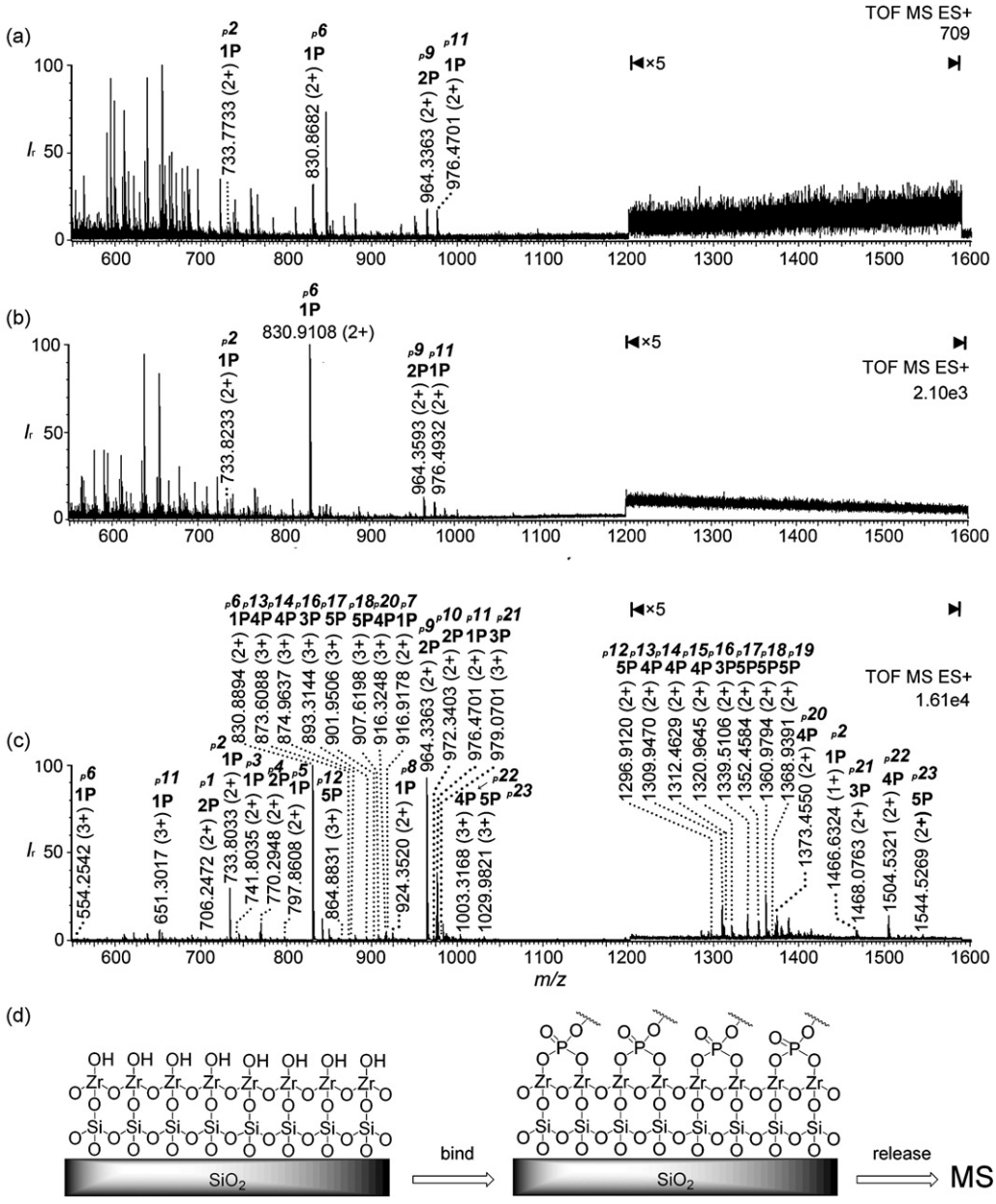

Fig. 5. Nano-ESI-TOF mass spectra for tryptic α-casein digests enriched by (a) 250 μg of MCF, (b) 500 μg of bulk ZrO_2, and (c) 250 μg of ZrO_2(24)/MCF. P indicates phosphate group. (d) Illustration of phosphopeptide binding to zirconia layer on the mesoporous silica surface.

Table 1
Endogenous phosphopeptides enriched from human serum.

Name	Phosphopeptide	Phosphosites	Mascot score	Known phosphorylations
Nephrocystin-3	AKpSIIIAECHSV	S3	28	No
Nephrocystin-3	DAKpSIIIAECHSV	S4	38	No
Thioredoxin domain-containing protein 1	VSEEEAESKEGTNK	T12	26	Yes
Eosinophil peroxidase	QAERCpS	S6	20	No
DNA polymerase zeta catalytic subunit	NpSLLLASLSIPQLD	S2	17	No
Transient receptor potential cation channel subfamily M member 1	QLpSLALAWNRV	S3	28	No
Folliculin-interacting protein 1	ISVSKLCpS	S8	15	No
Sterile alpha motif domain-containing protein 9	KPHGKIVGIKVpTN	T12	18	No
Pleckstrin homology domain-containing family M member 3	pSCFQVIFPQD	S1	18	No
PDZ domain-containing protein 4	AGPGLpSNSQEL	S6	16	No
Probable ubiquitin carboxyl-terminal hydrolase CYLD	PAKpSLTEIpST	S4, S9	20	No
Cylicin-1	DAKKIpTFpST	T6, S8	18	No

phopeptides on MCF silica (Fig. 5a). As seen from Fig. 5b, only 4 phosphorylated peptides could be found in elutions from bulk ZrO_2 particles. Compared with the bulk ZrO_2 and TiO_2 microparticles, ZrO_2(12)/MCF (Fig. 4c) and ZrO_2(24)/MCF (Fig. 5c) microspheres demonstrate much higher phosphopeptide-enrichment selectivity. Under acidic loading condition, the phosphate group on phosphopeptides can bind strongly with the coordinatively unsaturated Ti^{IV} species on the surface of bulk TiO_2 through bridging bidentate complex [15]. Based on the similar surface chemistry, we proposed the existence of the bridging bidentate complex between the phosphate group and the coordinatively unsaturated Zr^{IV} species on the surface of bulk ZrO_2. When ZrO_2 was dispersed on the mesoporous silica surface as uniform layer state, most of the zirconia species are in the form of isolated tetrahedral environment due to the formation of Si–O–Zr bonds. Compared with bulk ZrO_2, the bridging bidentate complex is favorable for the tetrahedral coordinated zirconia species on the mesoporous silica surface (Fig. 5d). The phosphate-active sites provided by highly dispersed coordinatively unsaturated Zr^{IV} species, together with the large surface area of mesoporous silica, guarantee the high specificity and high efficiency of ZrO_2(12, 24)/MCF for binding phosphopeptides. The high phosphopeptide recovery, especially for multi-phosphopeptides, is closely related to the high amount of coordinatively unsaturated Zr^{IV} species on the mesoporous silica surface.

3.2.2. Endogenous phosphopeptide enrichment from human serum

Isolation of phosphopeptides by zirconia layer on the mesoporous silica surface was demonstrated to be very specific and efficient using model phosphoprotein digests as the test samples. To demonstrate whether or not this approach could enrich phosphopeptides from complex sample, we decided to enrich the endogenous phosphopeptides, which exist in the native state, from human serum with ZrO_2(12)/MCF. The peptidome of human plasma has attracted increasing interest for its role in the elucidation of biological and pathological variation and discovery of useful biomarkers. Due to the huge complexity and extremely high dynamic range of human serum, analysis of human serum peptidome is a very challenging task and the endogenous phosphopeptides can hardly be found without enrichment. By titanium (IV) ion-immobilized mesoporous MCM-41 silica nanoparticles, four endogenous phosphopeptides could be enriched from human serum by centrifugation [21]. The synthesized MCM-41 has small pore size of 2 nm [41], which could restrict the phosphopeptide binding and release. In addition, centrifugation procedure would affect the recovery of the phosphopeptides. Here, ZrO_2(12)/MCF microspheres were explored in microcolumn to enrich phosphopeptides from human serum. Due to high specific phosphopeptides affinity of the zirconia layer on the mesoporous silica surface, together with large pore size of 22 nm and high surface area, 12 endogenous phosphorylated peptides could be specifically enriched with ZrO_2(12)/MCF from human serum even in presence of a huge amount of high-molecular-weight (HMW) proteins and non-phosphorylated peptides (Table 1).

4. Conclusions

Mesoporous MCF silica microspheres coated with highly dispersed ZrO_2 layer have been prepared and applied for enrichment of phosphopeptides. The novel enrichment strategy operated in microcolumn can enrich phosphopeptides from complex samples with high selectivity and efficiency. The superior enrichment performance of ZrO_2(12, 24)/MCF microspheres can be attributed to the high amount of coordinatively unsaturated zirconia species dispersed on the mesoporous silica surface, and unique textural structure, such as large surface area and flow-through pore structure. These ZrO_2 layer coated mesoporous silica microspheres present new opportunity in the development of highly selective and efficient materials for phosphopeptide enrichment.

Acknowledgements

This work was supported by the Foundation for Distinguished Young Scholars (No. 20825518) from National Natural Sciences Foundation of China and Major National Sci-Tech Projects (2009ZX09301-012, 2009ZX09308-001, and 2009ZX09501-011).

Appendix A. Supplementary data

Supplementary data associated with this article can be found, in the online version, at doi:10.1016/j.talanta.2010.07.050.

References

[1] L.N. Johnson, R.J. Lewis, Chem. Rev. 101 (2001) 2209–2242.
[2] K. Schmezle, F.M. White, Curr. Opin. Biotechnol. 17 (2006) 406–414.
[3] M.O. Collins, L. Yu, J.S. Choudhary, Proteomics 7 (2007) 2751–2768.
[4] B. Bodenmiller, L.N. Mueller, M. Mueller, B. Domon, R. Aebersold, Nat. Methods 4 (2007) 231–237.
[5] A. Pandey, A.V. Podtelejnikov, B. Blagoev, X.R. Bustelo, M. Mann, H.F. Lodish, Proc. Natl. Acad. Sci. U.S.A. 97 (2000) 179–184.
[6] S. Ficarro, O. Chertihin, V.A. Westbrook, F. White, F. Jayes, P. Kalab, J.A. Marto, J. Shabanowitz, J.C. Herr, D.F. Hunt, P.E. Visconti, J. Biol. Chem. 278 (2003) 11579–11589.
[7] B.A. Ballif, J. Villen, S.A. Beausoleil, D. Schwartz, S.P. Gygi, Mol. Cell. Proteomics 3 (2004) 1093–1101.
[8] S.A. Beausoleil, M. Jedrychowski, D. Schwartz, J.E. Elias, J. Villen, J.X. Li, M.A. Cohn, L.C. Cantley, S.P. Gygi, Proc. Natl. Acad. Sci. U.S.A. 101 (2004) 12130–12135.
[9] G.H. Han, M.L. Ye, H.J. Zhou, X.N. Jiang, S. Feng, X.G. Jiang, R.J. Tian, D.F. Wan, H.F. Zou, J.R. Gu, Proteomics 8 (2008) 1346–1361.
[10] D.C.A. Neville, C.R. Rozanas, E.M. Price, D.B. Gruis, A.S. Verkman, R.R. Townsend, Protein Sci. 6 (1997) 2436–2445.
[11] M.C. Posewitz, P. Tempst, Anal. Chem. 71 (1999) 2883–2892.
[12] T.S. Nuhse, A. Stensballe, O.N. Jensen, S.C. Peck, Mol. Cell. Proteomics 2 (2003) 1234–1243.

[13] A. Sano, H. Nakamura, Anal. Sci. 20 (2004) 565–566.
[14] M.W.H. Pinkse, P.M. Uitto, M.J. Hilhorst, B. Ooms, A.J.R. Heck, Anal. Chem. 76 (2004) 3935–3943.
[15] M.R. Larsen, T.E. Thingholm, O.N. Jensen, P. Roepstorff, T.J.D. Jorgensen, Mol. Cell. Proteomics 4 (2005) 873–886.
[16] H.K. Kweon, K. Hakansson, Anal. Chem. 78 (2006) 1743–1749.
[17] F. Wolschin, S. Wienkoop, W. Weckwerth, Proteomics 5 (2005) 4389–4397.
[18] M. Sturm, A. Leitner, J.H. Smatt, M. Linden, W. Lindner, Adv. Funct. Mater. 18 (2008) 2381–2389.
[19] C.T. Chen, Y.C. Chen, Anal. Chem. 77 (2005) 5912–5919.
[20] H.J. Zhou, R.J. Tian, M.L. Ye, S.Y. Xu, S. Feng, C.S. Pan, X.G. Jiang, X. Li, H.F. Zou, Electrophoresis 28 (2007) 2201–2215.
[21] L.H. Hu, H.J. Zhou, Y.H. Li, S.T. Sun, L.H. Guo, M.L. Ye, X.F. Tian, J.R. Gu, S.L. Yang, H.F. Zou, Anal. Chem. 81 (2009) 94–104.
[22] C.A. Nelson, J.R. Szczech, Q.G. Xu, M.J. Lawrence, S. Jin, Y. Ge, Chem. Commun. (2009) 6607–6609.
[23] T. Ono, M. Anpo, Y. Kubokawa, J. Phys. Chem. 90 (1986) 4780–4784.
[24] E.C. Alyea, L.J. Lakshmi, Z. Ju, Langmuir 13 (1997) 5621–5626.
[25] Y.Y. Huang, B.Y. Zhao, Y.C. Xie, Appl. Catal. A: Gen. 171 (1998) 65–73.
[26] J.Y. Ying, C.P. Mehnert, M.S. Wong, Angew. Chem. Int. Ed. 38 (1999) 56–77.
[27] K.W. Gallis, J.T. Araujo, K.J. Duff, J.G. Moore, C.C. Landry, Adv. Mater. 11 (1999) 1452–1455.
[28] M. Hartmann, Chem. Mater. 17 (2005) 4577–4593.
[29] E.W. Shin, J.S. Han, M. Jang, S.H. Min, J.K. Park, R.M. Rowell, Environ. Sci. Technol. 38 (2004) 912–917.
[30] J.J. Wan, K. Qian, L. Qiao, Y.H. Wang, J.L. Kong, P.Y. Yang, B.H. Liu, C.Z. Yu, Chem. Eur. J. 15 (2009) 2504–2508.
[31] P. Schmidt-Winkel, W.W. Lukens, D.Y. Zhao, P.D. Yang, B.F. Chmelka, G.D. Stucky, J. Am. Chem. Soc. 121 (1999) 254–255.
[32] P. Schmidt-Winkel, W.W. Lukens, P.D. Yang, D.I. Margolese, J.S. Lettow, J.Y. Ying, G.D. Stucky, Chem. Mater. 12 (2000) 686–696.
[33] Y. Han, S.S. Lee, J.Y. Ying, Chem. Mater. 19 (2007) 2292–2298.
[34] H.H. Wan, L. Liu, C.M. Li, X.Y. Xue, X.M. Liang, J. Colloid Interface Sci. 337 (2009) 420–426.
[35] C.K. Krishnan, T. Hayashi, M. Ogura, Adv. Mater. 20 (2008) 2131–2136.
[36] L.N. Wang, T. Qi, Y. Zhang, J.L. Chu, Micropor. Mesopor. Mater. 91 (2006) 156–160.
[37] M. Rainer, H. Sonderegger, R. Bakry, C.W. Huck, S. Morandell, L.A. Huber, D.T. Gjerde, G.K. Bonn, Proteomics 8 (2008) 4593–4602.
[38] M. Mazanek, G. Mituloviae, F. Herzog, C. Stingl, J.R.A. Hutchins, J.M. Peters, K. Mechtler, Nat. Protoc. 2 (2007) 1059–1069.
[39] Y. Kyono, N. Sugiyama, K. Imami, M. Tomita, Y. Ishihama, J. Proteome Res. 7 (2008) 4585–4593.
[40] N. Sugiyama, T. Masuda, K. Shinoda, A. Nakamura, M. Tomita, Y. Ishihama, Mol. Cell. Proteomics 6 (2007) 1103–1109.
[41] R.J. Tian, H. Zhang, M.L. Ye, X.G. Jiang, L.H. Hu, X. Li, X.H. Bao, H.F. Zou, Angew. Chem. Int. Ed. 46 (2007) 962–965.